DESY 16-035
Accepted for publication in Physics Letters B
March 2016

arXiv:1604.01280v1 [hep-ex] 5 Apr 2016

# Limits on the effective quark radius from inclusive *ep* scattering at HERA

ZEUS Collaboration

**Abstract**

The high-precision HERA data allows searches up to TeV scales for Beyond the Standard Model contributions to electron–quark scattering. Combined measurements of the inclusive deep inelastic cross sections in neutral and charged current $ep$ scattering corresponding to a luminosity of around 1 fb$^{-1}$ have been used in this analysis. A new approach to the beyond the Standard Model analysis of the inclusive $ep$ data is presented; simultaneous fits of parton distribution functions together with contributions of "new physics" processes were performed. Results are presented considering a finite radius of quarks within the quark form-factor model. The resulting 95% C.L. upper limit on the effective quark radius is $0.43 \cdot 10^{-16}$ cm.

# The ZEUS Collaboration

H. Abramowicz[25,u], I. Abt[20], L. Adamczyk[8], M. Adamus[31], S. Antonelli[2], V. Aushev[17], O. Behnke[10], U. Behrens[10], A. Bertolin[22], S. Bhadra[33], I. Bloch[11], E.G. Boos[15], I. Brock[3], N.H. Brook[29], R. Brugnera[23], A. Bruni[1], P.J. Bussey[12], A. Caldwell[20], M. Capua[5], C.D. Catterall[33], J. Chwastowski[7], J. Ciborowski[30,w], R. Ciesielski[10,f], A.M. Cooper-Sarkar[21], M. Corradi[1,a], R.K. Dementiev[19], R.C.E. Devenish[21], S. Dusini[22], B. Foster[13,m], G. Gach[8], E. Gallo[13,n], A. Garfagnini[23], A. Geiser[10], A. Gizhko[10], L.K. Gladilin[19], Yu.A. Golubkov[19], G. Grzelak[30], M. Guzik[8], C. Gwenlan[21], W. Hain[10], O. Hlushchenko[17], D. Hochman[32], R. Hori[14], Z.A. Ibrahim[6], Y. Iga[24], M. Ishitsuka[26], F. Januschek[10,g], N.Z. Jomhari[6], I. Kadenko[17], S. Kananov[25], U. Karshon[32], P. Kaur[4,b], D. Kisielewska[8], R. Klanner[13], U. Klein[10,h], I.A. Korzhavina[19], A. Kotański[9], U. Kötz[10], N. Kovalchuk[13], H. Kowalski[10], B. Krupa[7], O. Kuprash[10,i], M. Kuze[26], B.B. Levchenko[19], A. Levy[25], S. Limentani[23], M. Lisovyi[10,j], E. Lobodzinska[10], B. Löhr[10], E. Lohrmann[13], A. Longhin[22,t], D. Lontkovskyi[10], O.Yu. Lukina[19], I. Makarenko[10], J. Malka[10], A. Mastroberardino[5], F. Mohamad Idris[6,d], N. Mohammad Nasir[6], V. Myronenko[10,k], K. Nagano[14], T. Nobe[26], R.J. Nowak[30], Yu. Onishchuk[17], E. Paul[3], W. Perlański[30,x], N.S. Pokrovskiy[15], A. Polini[1], M. Przybycień[8], P. Roloff[10,l], M. Ruspa[28], D.H. Saxon[12], M. Schioppa[5], U. Schneekloth[10], T. Schörner-Sadenius[10], L.M. Shcheglova[19], R. Shevchenko[17,q,r], O. Shkola[17], Yu. Shyrma[16], I. Singh[4,c], I.O. Skillicorn[12], W. Słomiński[9,e], A. Solano[27], L. Stanco[22], N. Stefaniuk[10], A. Stern[25], P. Stopa[7], D. Sukhonos[17], J. Sztuk-Dambietz[13,g], E. Tassi[5], K. Tokushuku[14,o], J. Tomaszewska[30,y], T. Tsurugai[18], M. Turcato[13,g], O. Turkot[10,k], T. Tymieniecka[31], A. Verbytskyi[20], W.A.T. Wan Abdullah[6], K. Wichmann[10,k], M. Wing[29,v], S. Yamada[14], Y. Yamazaki[14,p], N. Zakharchuk[17,s], A.F. Żarnecki[30], L. Zawiejski[7], O. Zenaiev[10], B.O. Zhautykov[15], D.S. Zotkin[19]

[1] *INFN Bologna, Bologna, Italy* [A]

[2] *University and INFN Bologna, Bologna, Italy* [A]

[3] *Physikalisches Institut der Universität Bonn, Bonn, Germany* [B]

[4] *Panjab University, Department of Physics, Chandigarh, India*

[5] *Calabria University, Physics Department and INFN, Cosenza, Italy* [A]

[6] *National Centre for Particle Physics, Universiti Malaya, 50603 Kuala Lumpur, Malaysia* [C]

[7] *The Henryk Niewodniczanski Institute of Nuclear Physics, Polish Academy of Sciences, Krakow, Poland* [D]

[8] *AGH-University of Science and Technology, Faculty of Physics and Applied Computer Science, Krakow, Poland* [D]

[9] *Department of Physics, Jagellonian University, Krakow, Poland*

[10] *Deutsches Elektronen-Synchrotron DESY, Hamburg, Germany*

[11] *Deutsches Elektronen-Synchrotron DESY, Zeuthen, Germany*

[12] *School of Physics and Astronomy, University of Glasgow, Glasgow, United Kingdom* [E]

[13] *Hamburg University, Institute of Experimental Physics, Hamburg, Germany* [F]

[14] *Institute of Particle and Nuclear Studies, KEK, Tsukuba, Japan* [G]

[15] *Institute of Physics and Technology of Ministry of Education and Science of Kazakhstan, Almaty, Kazakhstan*

[16] *Institute for Nuclear Research, National Academy of Sciences, Kyiv, Ukraine*

[17] *Department of Nuclear Physics, National Taras Shevchenko University of Kyiv, Kyiv, Ukraine*

[18] *Meiji Gakuin University, Faculty of General Education, Yokohama, Japan* [G]

[19] *Lomonosov Moscow State University, Skobeltsyn Institute of Nuclear Physics, Moscow, Russia* [H]

[20] *Max-Planck-Institut für Physik, München, Germany*

[21] *Department of Physics, University of Oxford, Oxford, United Kingdom* [E]

[22] *INFN Padova, Padova, Italy* [A]

[23] *Dipartimento di Fisica e Astronomia dell' Università and INFN, Padova, Italy* [A]

[24] *Polytechnic University, Tokyo, Japan* [G]

[25] *Raymond and Beverly Sackler Faculty of Exact Sciences, School of Physics, Tel Aviv University, Tel Aviv, Israel* [I]

[26] *Department of Physics, Tokyo Institute of Technology, Tokyo, Japan* [G]

[27] *Università di Torino and INFN, Torino, Italy* [A]

[28] *Università del Piemonte Orientale, Novara, and INFN, Torino, Italy* [A]

[29] *Physics and Astronomy Department, University College London, London, United Kingdom* [E]

[30] *Faculty of Physics, University of Warsaw, Warsaw, Poland*

[31] *National Centre for Nuclear Research, Warsaw, Poland*

[32] *Department of Particle Physics and Astrophysics, Weizmann Institute, Rehovot, Israel*

[33] *Department of Physics, York University, Ontario, Canada M3J 1P3* [J]

[A] supported by the Italian National Institute for Nuclear Physics (INFN)

[B] supported by the German Federal Ministry for Education and Research (BMBF), under contract No. 05 H09PDF

[C] supported by HIR grant UM.C/625/1/HIR/149 and UMRG grants RU006-2013, RP012A-13AFR and RP012B-13AFR from Universiti Malaya, and ERGS grant ER004-2012A from the Ministry of Education, Malaysia

[D] supported by the National Science Centre under contract No. DEC-2012/06/M/ST2/00428

[E] supported by the Science and Technology Facilities Council, UK

[F] supported by the German Federal Ministry for Education and Research (BMBF), under contract No. 05h09GUF, and the SFB 676 of the Deutsche Forschungsgemeinschaft (DFG)

[G] supported by the Japanese Ministry of Education, Culture, Sports, Science and Technology (MEXT) and its grants for Scientific Research

[H] supported by RF Presidential grant N 3042.2014.2 for the Leading Scientific Schools

[I] supported by the Israel Science Foundation

[J] supported by the Natural Sciences and Engineering Research Council of Canada (NSERC)

[a] now at INFN Roma, Italy

[b] now at Sant Longowal Institute of Engineering and Technology, Longowal, Punjab, India

[c] now at Sri Guru Granth Sahib World University, Fatehgarh Sahib, India

[d] also at Agensi Nuklear Malaysia, 43000 Kajang, Bangi, Malaysia

[e] partially supported by the Polish National Science Centre projects DEC-2011/01/B/ST2/03643 and DEC-2011/03/B/ST2/00220

[f] now at Rockefeller University, New York, NY 10065, USA

[g] now at European X-ray Free-Electron Laser facility GmbH, Hamburg, Germany

[h] now at University of Liverpool, United Kingdom

[i] now at Tel Aviv University, Isreal

[j] now at Physikalisches Institut, Universität Heidelberg, Germany

[k] supported by the Alexander von Humboldt Foundation

[l] now at CERN, Geneva, Switzerland

[m] Alexander von Humboldt Professor; also at DESY and University of Oxford

[n] also at DESY

[o] also at University of Tokyo, Japan

[p] now at Kobe University, Japan

[q] member of National Technical University of Ukraine, Kyiv Polytechnic Institute, Kyiv, Ukraine

[r] now at DESY CMS group

[s] now at DESY ATLAS group

[t] now at LNF, Frascati, Italy

[u] also at Max Planck Institute for Physics, Munich, Germany, External Scientific Member

[v] also supported by DESY and the Alexander von Humboldt Foundation

[w] also at Łódź University, Poland

[x] member of Łódź University, Poland

[y] now at Polish Air Force Academy in Deblin

# 1 Introduction

Precision measurements of deep inelastic $e^{\pm}p$ scattering (DIS) cross sections at high values of negative four-momentum-transfer squared, $Q^2$, allow searches for contributions beyond the Standard Model (BSM), even far beyond the centre-of-mass energy of the $e^{\pm}p$ interactions. For many "new physics" scenarios, cross sections can be affected by new kinds of interactions in which virtual BSM particles are exchanged. The cross sections would also be influenced were quarks to have a finite radius. As the HERA kinematic range is assumed to be far below the scale of the new physics, all such BSM interactions can be approximated as contact interactions (CI). In all cases, deviations of the observed cross section from the Standard Model (SM) prediction are searched for in $ep$ scattering at the highest available $Q^2$. The predictions are calculated using parton distribution function (PDF) parameterisations of the proton.

The H1 and ZEUS collaborations measured inclusive $e^{\pm}p$ scattering cross sections at HERA from 1994 to 2000 (HERA I) and from 2002 to 2007 (HERA II), collecting together a total integrated luminosity of about $1\,\mathrm{fb}^{-1}$. All inclusive data were recently combined [1] to create one consistent set of neutral current (NC) and charged current (CC) cross-section measurements for $e^{\pm}p$ scattering with unpolarised beams. The inclusive cross sections were used as input to a QCD analysis within the DGLAP formalism, resulting in a PDF set denoted as HERAPDF2.0. Due to the high precision and consistency of the input data, HERAPDF2.0 can be used to calculate SM predictions with small uncertainties. A search for BSM contributions in the data should take into account the possibility that the PDF set may already have been biased by partially or totally absorbing previously unrecognised BSM contributions.

In the ZEUS CI analysis of HERA I $e^{\pm}p$ data [2], the uncertainties on the PDFs used were a dominant source of systematic error. Estimated uncertainties of the parton densities were used to smear model predictions in the limit-setting procedure. Such an approach was valid as the CTEQ5D parameterisation [3, 4] used for calculating model predictions included only 1994 HERA data in addition to many other data sets. The limits were dominated by statistical uncertainties. For the CI analysis presented here, in which the data are identical to those used for the HERAPDF2.0 determination and the statistical uncertainties are no longer dominant, a new procedure to set limits on the BSM model contributions is required. In this analysis BSM contributions and the QCD evolution are fitted simultaneously. Results of a search for a finite quark radius are presented within the formalism of the quark form-factor model [5].

## 2 QCD analysis

The QCD analysis presented in this paper was performed similarly to that for the HERAPDF2.0 determination [1]. It was used to predict cross sections without BSM contributions. The HERA combined data on inclusive $e^{\pm}p$ scattering [1] were used as input to the perturbative QCD (pQCD) analysis. Only cross sections with $Q^2 \geqslant 3.5\,\mathrm{GeV}^2$ were used. A fit to the data, resulting in a set of PDFs, was obtained by solving the DGLAP evolution equations at NLO in the $\overline{\mathrm{MS}}$ scheme. This was done using the programme QCDNUM [6] within the HERAFitter framework [7]. For the PDF parameterisation, the approach adopted in the HERAPDF2.0 study [1] was followed. The PDFs of the proton were described at a starting scale of 1.9 $\mathrm{GeV}^2$ in terms of 14 parameters. These parameters were fit to the data using a $\chi^2$ method, taking into account statistical uncertainties, as well as uncorrelated and correlated systematic uncertainties on the experimental data. The corresponding $\chi^2$ formula is:

$$\chi^2\left(\boldsymbol{m},\boldsymbol{s}\right) = \sum_i \frac{\left[m^i + \sum_j \gamma_j^i m^i s_j - \mu_0^i\right]^2}{\left(\delta_{i,\mathrm{stat}}^2 + \delta_{i,\mathrm{uncor}}^2\right)\,(\mu_0^i)^2} + \sum_j s_j^2 \quad , \tag{1}$$

where $\mu_0^i$ is the measured cross-section value at the point $i$. The quantities $\gamma_j^i$, $\delta_{i,\mathrm{stat}}$ and $\delta_{i,\mathrm{uncor}}$ are the relative correlated systematic, relative statistical and relative uncorrelated systematic uncertainties of the input data, respectively. The vector $\boldsymbol{m}$ represents the set of pQCD cross-section predictions $m^i$ and the components $s_j$ of the vector $\boldsymbol{s}$ represent the correlated systematic shifts of the cross sections (given in units of $\gamma_j^i$). The summations extend over all data points $i$ and all correlated systematic uncertainties $j$.

The $\chi^2$ formula used in this analysis differs from that of HERAPDF2.0 study [1] in order to facilitate the production of data replicas within the HERAFitter framework [7], see Section 4. The resulting sets of PDFs, referred to as ZRqPDF in the following, are nevertheless in good agreement with HERAPDF2.0.

The experimental uncertainties on the predictions from ZRqPDF were determined with the criterion $\Delta\chi^2 = 1$. The uncertainties due to the choice of model settings and the form of the parameterisation were evaluated as for HERAPDF2.0.

## 3 Quark form factor

One of the possible parameterisations of deviations from SM predictions in $ep$ scattering is achieved by assigning an effective finite radius to electrons and/or quarks while assuming the SM gauge bosons remain point-like and their couplings unchanged. The expected modification of the SM cross section can be described using a semi-classical form-factor

approach [5]. If the expected deviations are small, the SM predictions for the cross sections are modified, approximately, to:

$$\frac{d\sigma}{dQ^2} = \frac{d\sigma^{\mathrm{SM}}}{dQ^2}\left(1-\frac{R_e^2}{6}Q^2\right)^2\left(1-\frac{R_q^2}{6}Q^2\right)^2 , \quad (2)$$

where $R_e^2$ and $R_q^2$ are the mean-square radii of the electron and the quark, respectively, related to new BSM energy scales. In the present analysis, only the possible finite spatial distribution of the quark was considered and the electron was assumed to be point-like ($R_e^2 \equiv 0$). Both positive and negative values of $R_q^2$ were considered. Negative values of $R_q^2$ can be obtained if a charge distribution is assumed which changes sign as a function of the radius. The term "quark radius" is only one possible interpretation of BSM effects parameterised as form factors.

The QCD analysis described in the previous section was extended by introducing $R_q^2$ as an additional model parameter and modifying all $e^{\pm}p$ DIS cross-section predictions according to Eq. 2. Values for $R_q^2$ were extracted using a $\chi^2$-minimisation procedure, where all PDF parameters were also simultaneously fit; $R_q^2$ was treated as a test statistic to be used for limit setting. The value of this test statistic for the data is $R_q^{2\,\mathrm{Data}} = -0.2 \cdot 10^{-33}$ cm$^2$. The probability distributions for $R_q^2$ were determined as described in the next section.

# 4 Limit-setting procedure

The limit on the effective quark-radius squared, $R_q^2$, is derived in a frequentist approach [8] using the technique of replicas. Replicas are sets of cross-section values that are generated by varying all cross sections randomly according to their known uncertainties. For the analysis presented here, multiple replica sets were used, each covering cross-section values on all points of the $x, Q^2$ grid used in the QCD fit. For an assumed true value of the quark-radius squared, $R_q^{2\,\mathrm{True}}$, replica data sets were created by taking the reduced cross sections calculated from the ZRqPDF fit and scaling them with the quark form factor, Eq. 2, with $R_q^2 = R_q^{2\,\mathrm{True}}$. This results in a set of cross-section values $m_0^i$ for the assumed true quark-radius squared, $R_q^{2\,\mathrm{True}}$. The values of $m_0^i$ were then varied randomly within statistical and systematic uncertainties taken from the data, taking correlations into account. All uncertainties were assumed to follow a Gaussian distribution[1]. For each replica, the generated value of the cross section at the point $i$, $\mu^i$, was calculated as:

$$\mu^i = \left[m_0^i + \sqrt{\delta_{i,\mathrm{stat}}^2 + \delta_{i,\mathrm{uncor}}^2}\cdot\mu_0^i\cdot r_i\right]\cdot\left(1+\sum_j \gamma_j^i \cdot r_j\right) , \quad (3)$$

[1] It was verified that using a Poisson probability distribution for producing replicas at high $Q^2$, where the event samples are small, and using the $\chi^2$ minimisation for these data did not significantly change the probability distributions for the fitted parameter values.

where variables $r_i$ and $r_j$ represent random numbers from a normal distribution for each data point $i$ and for each source of correlated systematic uncertainty $j$, respectively.

The approach adopted was to generate sets of replicas that were used to test the hypothesis that the cross sections were modified by a fixed $R_q^2$ value according to Eq. 2. The value of $R_q^{2\,\mathrm{Data}}$ determined by the fit to the data themselves was taken as a test statistic, to which values from fits to replicas, $R_q^{2\,\mathrm{Fit}}$, could be compared. Positive (negative) $R_q^{2\,\mathrm{True}}$ values that, in more than 95% of the replicas, result in the fitted radius squared value, $R_q^{2\,\mathrm{Fit}}$, greater than (less than) that obtained for the data, $R_q^{2\,\mathrm{Data}}$, were excluded at the 95% C.L. The details of these procedures are described below.

To set the limit, a number of MC replica cross-section sets for each value of $R_q^{2\,\mathrm{True}}$ was used for a QCD fit with the PDF parameters and the quark radius as free parameters, yielding a distribution of the fitted values of the quark radius, $R_q^{2\,\mathrm{Fit}}$. The $\chi^2$ formula of Eq. 1, with the measured cross-section values, $\mu_0^i$, in the numerator of the first term replaced by the generated values of the replica, $\mu^i$, was used for fitting $R_q^2$ and the PDF parameters.

In a last step, the probability of obtaining a $R_q^{2\,\mathrm{Fit}}$ value smaller than that obtained for the actual data, $\mathrm{Prob}(R_q^{2\,\mathrm{Fit}} < R_q^{2\,\mathrm{Data}})$, was plotted as a function of $R_q^{2\,\mathrm{True}}$, for positive $R_q^{2\,\mathrm{True}}$ values, as shown in Fig. 1. The probability distribution was interpolated to calculate the $R_q^2$ value corresponding to the 95% C.L. upper limit. About 5000 Monte Carlo replicas were generated for each value of $R_q^{2\,\mathrm{True}}$ resulting in a relative statistical uncertainty of the extracted limit of about 0.3%. The corresponding plot for negative $R_q^{2\,\mathrm{True}}$ values is shown in Fig. 2.

As a cross check, the limits on $R_q^2$ were also estimated from the simultaneous PDF and $R_q^2$ fit to the data by looking at the variation of the $\chi^2$ value minimised with respect to the PDF parameters when changing the $R_q^2$ value. Both limits are in good agreement with the results based on the Monte Carlo replicas. The limit-setting procedure was also repeated for different model and parameter settings, considered as systematic checks in the HERAPDF2.0 analysis [1]. The resulting variations of the limits on $R_q^2$ are negligible.

# 5 Results

The results of the limit-setting procedure using the simultaneous fit to PDF parameters and $R_q^2$, based on sets of Monte Carlo replicas testing the possible cross-section modifications due to a quark form factor, yield the 95% C.L. limits on the effective quark radius of

$$-(0.47 \cdot 10^{-16}\,\mathrm{cm})^2 \;<\; R_q^2 \;<\; (0.43 \cdot 10^{-16}\,\mathrm{cm})^2 \,.$$

Taking into account the possible influence of quark radii on the PDF parameters is necessary as demonstrated in Figs. 1 and 2, because the limits that would be obtained for

fixed PDF parameters are too strong by about 10%. The limits are consistent with the estimated experimental sensitivity, calculated as the median of the limit distribution for the SM replicas, corresponding to a quark radius of $0.45 \cdot 10^{-16}$ cm (for both positive and negative $R_q^2$). Cross-section deviations given by Eq. 2, corresponding to the presented 95% C.L. exclusion limits, are compared to the combined HERA high-$Q^2$ NC and CC DIS data in Figs. 3 and 4, respectively.

The 95% C.L. upper limit for the quark radius presented here is almost a factor of two better than the previous ZEUS limit of $0.85 \cdot 10^{-16}$ cm, based on the HERA I data [2]. The present result improves the limit set in $ep$ scattering by the H1 collaboration [9] ($R_q < 0.65 \cdot 10^{-16}$ cm) and is similar to the limit presented by the L3 collaboration ($R_q < 0.42 \cdot 10^{-16}$ cm), based on quark-pair production at LEP2 [10]. It is important to remember that the possible BSM physics parameterised by the $R_q$ at LEP and HERA can be very different, so that the LEP and HERA limits are largely complementary. The limit on negative $R_q^2$ values presented here is an improvement compared to the published ZEUS limit of $R_q^2 > -(1.06 \cdot 10^{-16}\,\text{cm})^2$.

# 6 Conclusions

The HERA combined measurement of inclusive deep inelastic cross sections in neutral and charged current $e^{\pm}p$ scattering was used to set limits on possible deviations from the Standard Model due to a finite radius of the quarks. The limit-setting procedure was based on a simultaneous fit of PDF parameters and the quark radius. The resulting 95% C.L. limits for the quark radius are

$$-(0.47 \cdot 10^{-16}\,\text{cm})^2 \; < \; R_q^2 \; < \; (0.43 \cdot 10^{-16}\,\text{cm})^2 \; .$$

This result is competitive with a determination from LEP2 and substantially improves previous HERA limits.

# Acknowledgements

We appreciate the contributions to the construction, maintenance and operation of the ZEUS detector of many people who are not listed as authors. The HERA machine group and the DESY computing staff are especially acknowledged for their success in providing excellent operation of the collider and the data-analysis environment. We thank the DESY directorate for their strong support and encouragement.

# References


[1] H1 and ZEUS Collaborations, H. Abramowicz et al., Eur. Phys. J. C 75 (2015) 580.

[2] ZEUS Collaboration, S. Chekanov et al., Phys. Lett. B 591 (2004) 23.

[3] CTEQ Collaboration, H.L. Lai et al., Eur. Phys. J. C 12 (2000) 375.

[4] CTEQ Collaboration, H.L. Lai et al., Phys. Rev. D 55 (1997) 1280.

[5] G. Kopp et al., Z. Phys. C 65 (1995) 545.

[6] M. Botje, Comp. Phys. Comm. 182 (2011) 490.

[7] S. Alekhin et al., Eur. Phys. J. C 75 (2015) 304.

[8] R.D. Cousins, Am. J. Phys. 63 (1995) 398.

[9] H1 Collaboration, F.D. Aaron et al., Phys. Lett. B 705 (2011) 52.

[10] L3 Collaboration, M. Acciarri et al., Phys. Lett. B 489 (2000) 81.

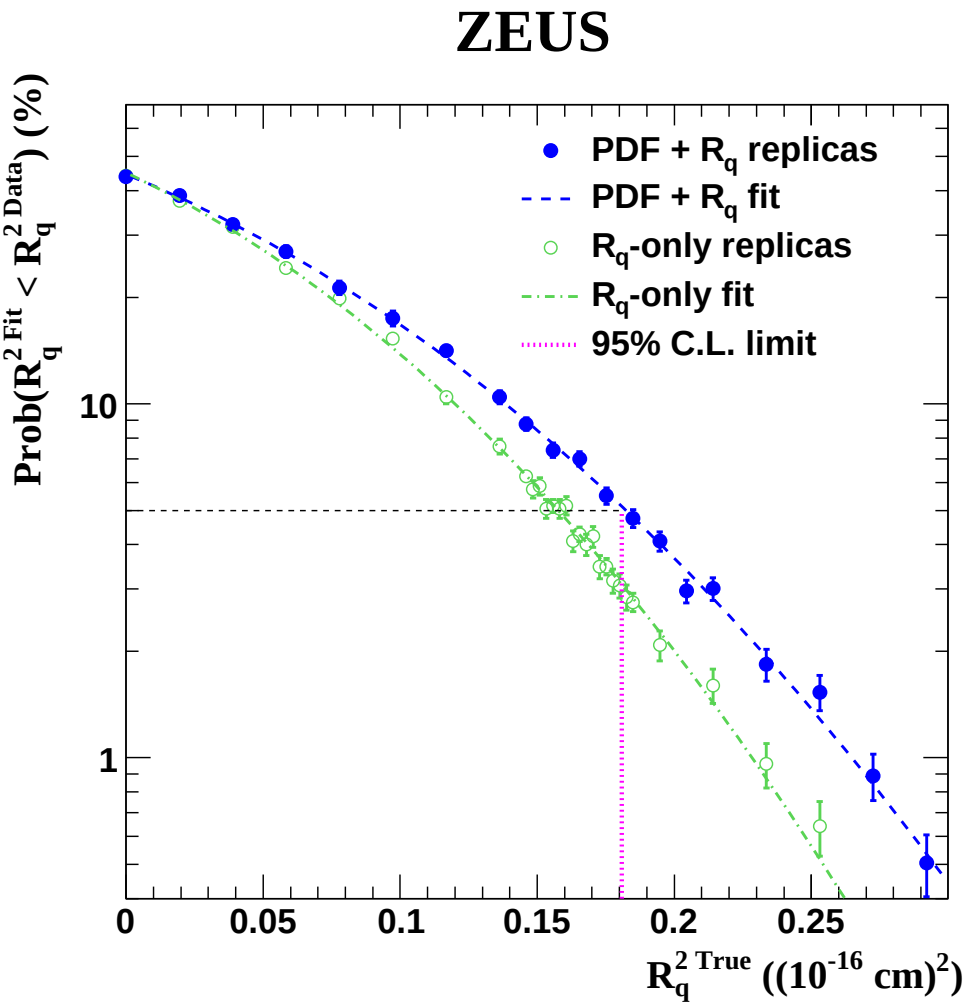



**Figure 1:** *The probability of obtaining $R_q^{2\,Fit}$ values smaller than that obtained for the actual data, $R_q^{2\,Data}$, calculated from Monte Carlo replicas, as a function of the assumed value for the quark-radius squared, $R_q^{2\,True}$. Points with statistical error bars represent Monte Carlo replica sets generated for different values of $R_q^{2\,True}$. The solid circles correspond to the results obtained from the simultaneous fit of $R_q^2$ and PDF parameters (PDF+$R_q$). For comparison, the open circles represent the dependence obtained when fixing the PDF parameters to the ZRqPDF values ($R_q$-only). The dashed line and the dashed–dotted line represent the cumulative Gaussian distributions fitted to the PDF+$R_q$ and $R_q$-only replica points, respectively. The vertical line represents the 95% C.L. upper limit on $R_q^2$.*

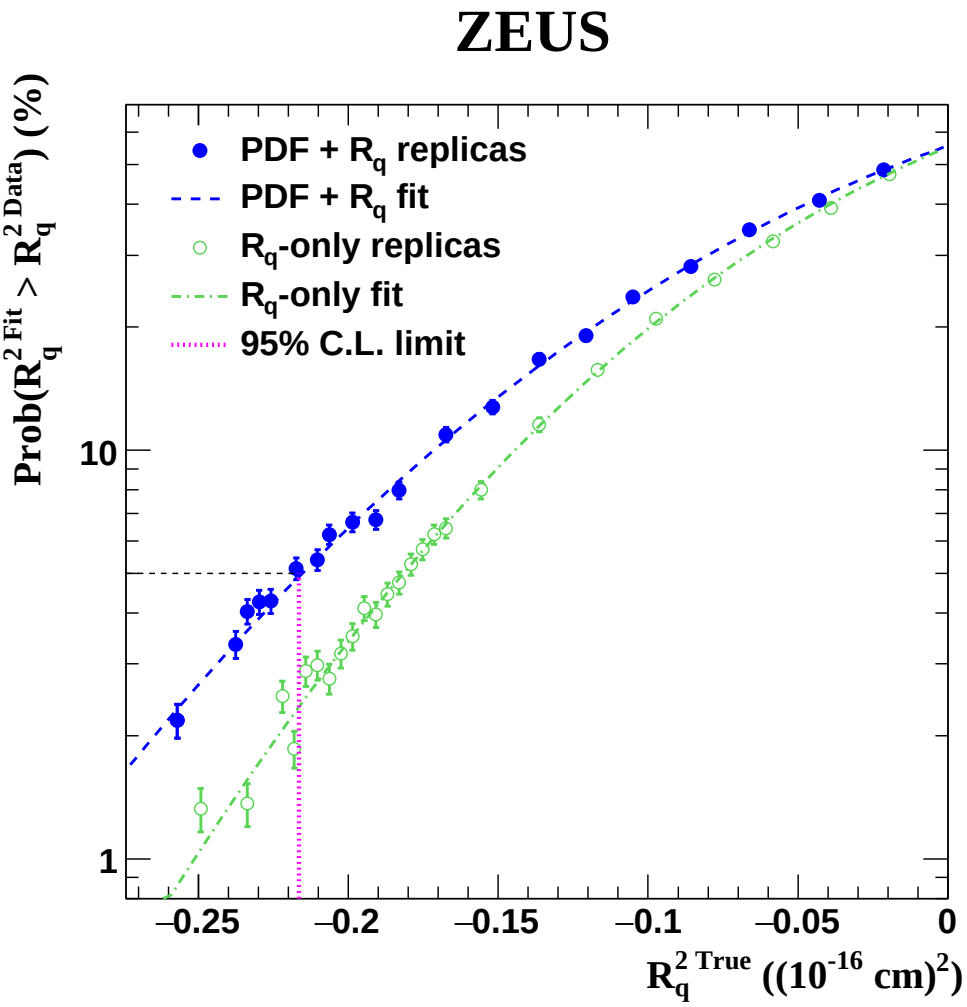



**Figure 2:** *The probability of obtaining $R_q^{2\,Fit}$ values larger than that obtained for the actual data, $R_q^{2\,Data}$, calculated from Monte Carlo replicas, as a function of the assumed value for the quark-radius squared, $R_q^{2\,True}$. Other details as for Fig. 1.*

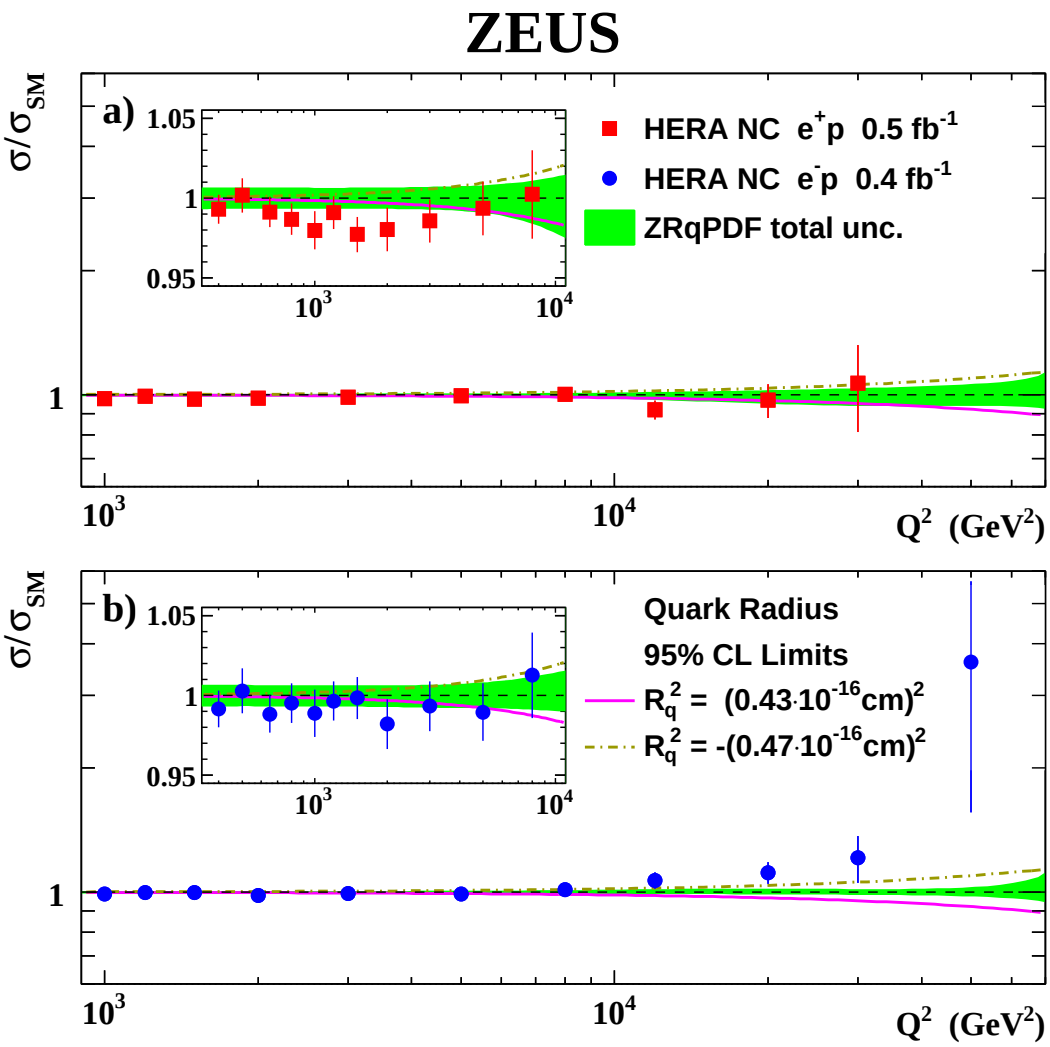



**Figure 3:** *Combined HERA (a) $e^+p$ and (b) $e^-p$ NC DIS data compared to the 95% C.L. exclusion limits on the effective mean-square radius of quarks. Also shown are the expectations calculated using the ZRqPDF parton distributions. The bands represent the total uncertainty on the predictions. The insets show the comparison in the $Q^2 < 10^4$ $GeV^2$ region with a linear ordinate scale.*

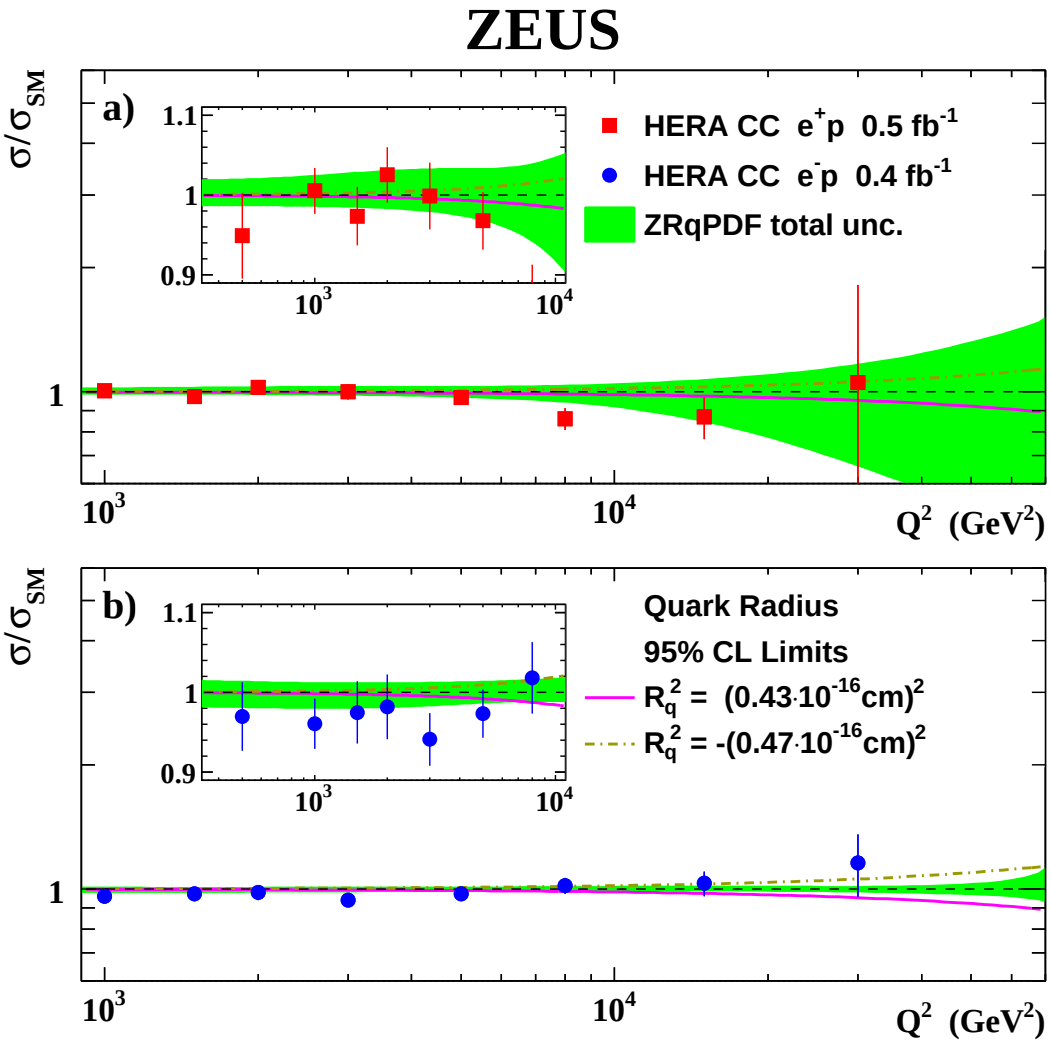



**Figure 4:** *Combined HERA (a) $e^+p$ and (b) $e^-p$ CC DIS data compared to the 95% C.L. exclusion limits on the effective mean-square radius of quarks. Other details as for Fig. 3.*